

# Dissolution of Styrene–Butadiene Block Copolymers in Biodiesel

Ying Zhang, Surya K. Mallapragada, Balaji Narasimhan

Department of Chemical and Biological Engineering, Iowa State University, 2035 Sweeney Hall, Ames, Iowa 50011-2230

Received 9 January 2010; accepted 2 April 2010

DOI 10.1002/app.32572

Published online 7 June 2010 in Wiley InterScience (www.interscience.wiley.com).

**ABSTRACT:** The goal of this study was to investigate the dissolution behavior of styrene–butadiene block copolymers in biodiesel with an eye toward developing a promising method of plastic waste disposal by burning them with engine fuel. The dissolution kinetics was investigated by high-throughput Fourier transform infrared microscopy, and the effect of the dissolution temperature on the kinetics was quantified. The activation energy of dissolution was estimated from the dissolution kinetics, and it was shown that the styrene–butadiene copolymers had higher activation energies than the neat polystyrene. The experimental studies were complemented by molecular dynamics simulations to calculate the Flory–Huggins

parameters between styrene and butadiene polymers and methyl esters. The shear viscosity of the block copolymer solutions in biodiesel was measured to ascertain their suitability as fuel mixtures. Finally, the mechanical properties of the styrene–butadiene block copolymers were compared to that of poly(ethylene terephthalate). Together, these studies suggest that styrene–butadiene block copolymers may offer a more environmentally friendly alternative to poly(ethylene terephthalate). © 2010 Wiley Periodicals, Inc. *J Appl Polym Sci* 118: 1859–1866, 2010

**Key words:** block copolymers; molecular modeling; recycling; waste

## INTRODUCTION

The last 50 years have witnessed explosive growth in the plastics industry. Today, plastics are widely used in many important everyday applications, such as packaging, clothing, household appliances, automotive products, computers, and transportation.<sup>1,2</sup> Despite the tremendous conveniences that plastics provide, the accumulation of waste plastics results in serious environmental and economic consequences. Plastics account for 11.7 wt % of the municipal solid waste generated in the United States, which in 2006 amounted to about 30 million tons.<sup>3</sup> This is in addition to the 7.6 billion tons of industrial waste, which contains plastics, that is generated annually in the United States.<sup>4</sup> In this context, there is an urgent need to develop methods to enable the conversion of waste plastics to useful products or energy. Waste plastics can be viewed as an enormous potential resource, which, with the correct treatment, can be reused or serve as hydrocarbon raw material or fuel.<sup>5</sup> For example, the dissolution of waste plastics

has emerged as a successful process for the treatment of unsorted plastics for recycling.<sup>6</sup> Additionally, a waste-plastics-to-energy process would have great utility for the military at a forward base in minimizing the transport logistics of hauling waste and supplying fuel.

Recently, our group showed that some waste plastics are soluble in biodiesel<sup>7</sup> and that these solutions could be used to power diesel engines. The waste plastics in these studies were polystyrene (PS) and low-density polyethylene. Biodiesel (which is a blend of methyl esters) is produced from domestic, renewable resources so that it can act as a clean-burning alternative fuel.<sup>8</sup> The lubricity of biodiesel, compared to regular diesel, can make polymer–biodiesel solutions more amenable for use as engine fuels.<sup>9,10</sup> The dissolution behavior of PS and low-density polyethylene in biodiesel has been characterized by investigations of its dissolution kinetics and shear viscosity and by molecular dynamic simulations. The dissolution process occurred before the fuel was burned in a diesel engine and involved the premixing and commingling of the waste plastics. These studies clearly demonstrated the feasibility of the dissolution of waste plastics in biodiesel. This work was complemented by the development of high-throughput methods to investigate polymer dissolution in solvents.<sup>11</sup> A rapid prototyping method was developed to fabricate multiwell substrates, which were used together with

Correspondence to: B. Narasimhan (nbalaji@iastate.edu).

Contract grant sponsor: U.S. Government; contract grant number: Other Transaction DAAE30-01-9-0800.

Contract grant sponsor: General Atomics and West Central Cooperative/Renewable Energy Group.

high-throughput Fourier transform infrared (FTIR) microscopy to simultaneously study the effects of the temperature and polymer molecular weight on the dissolution kinetics of PS in biodiesel. The results were consistent with conventional gravimetric studies and provided a novel and convenient method to rapidly evaluate the effect of multiple parameters on the dissolution process.

This study focused on the dissolution behavior of styrene-butadiene block copolymers in biodiesel. Styrene-butadiene block copolymers are used in a wide variety of applications because of their outstanding impact resistance, transparency, and low density.<sup>12–14</sup> These properties enable facile processing of these materials into complex three-dimensional shapes such as bottles. The goal of this study was to identify conditions under which styrene-butadiene block copolymers were soluble in biodiesel to lay the foundation for the consideration of these materials as potential replacements for poly(ethylene terephthalate) (PET). FTIR microscopy and molecular modeling were used to characterize the dissolution kinetics. The rheological and mechanical properties of the block copolymers were measured and compared to those of PET.

## EXPERIMENTAL

### Materials and characterization

Two kinds of styrene-butadiene block copolymers were used in these studies. Styrolux 684D [S1; number-average molecular weight ( $M_n$ ) = 150 kg/mol, polydispersity index (PDI) = 1.2, glass-transition temperature ( $T_g$ ) = 82°C, PS weight fraction = 0.74] and K-Resin (S2;  $M_n$  = 120 kg/mol, PDI = 1.4,  $T_g$  = 82°C, PS weight fraction = 70–85%) copolymers were provided by BASF (Florham Park, NJ) and Chevron Phillips (The Woodlands, TX), respectively. PS samples ( $M_n$  = 140 kg/mol, PDI = 1.7,  $T_g$  = 105°C) were provided by General Atomics, Inc. (San Diego, CA). PET samples used for the mechanical tests were obtained from commercial 2-L soda bottles. Biodiesel was supplied by West Central (Ralston, IA). The molar composition of biodiesel was 11.17% methyl palmitate, 4.07% methyl stearate, 23.80% methyl oleate, 53.03% methyl linoleate, and 7.10% methyl linolenate. The NOA 81 thiolene resin was purchased from Norland Products, Inc. (Cranbury, NJ). Double-polished silicon (100) wafers 5.08 cm in diameter were purchased from University Wafer (South Boston, MA).

A Nicolet 6700 FTIR spectrometer (Thermo Fisher, Madison, WI) was used to characterize the molecular structures of the copolymers and methyl esters. The polymer films for FTIR testing were prepared by the casting of solutions of 5 wt % polymer/

toluene onto glass plates and evaporation of the solvent, whereas the biodiesel samples were prepared by the coating of a small amount of biodiesel onto a 2 mm thick CaF<sub>2</sub> substrate. The FTIR measurements were conducted at a resolution of 8 cm<sup>-1</sup> by the averaging of 32 scans with a mercury cadmium telluride detector.

### Multiwell substrate fabrication

Multiwell array substrates were designed and fabricated according to a recently developed rapid prototyping technique based on the contact lithography of multifunctional thiolene resins.<sup>15–17</sup> The photomask consisted of a 4 × 4 grid (rectangular shape with dimensions of 7.5 × 5 mm<sup>2</sup>) and was designed with MS Word and printed on a transparency with a 1200-dpi resolution laser printer. The mask was then taped to a glass plate. Standard 4-in. i.d. plastic Petri dishes were used as the platform for the overall photolithography process. Approximately 5–10 mL of NOA 81 was poured into each Petri dish, and the mask-substrate assembly was carefully positioned over the thiolene. A flood 365-nm UV source (Solitec, Inc., Santa Clara, CA) was used to image the mask pattern onto the photoresist at an intensity of 15 mW/cm<sup>2</sup>. The whole setup was removed from UV radiation after 5 min of exposure. Acetone was then used to wash away the uncured optical adhesive. Subsequently, the patterned multiwell was gently stripped from the glass substrate and placed on a silicon wafer after the bottom side of the multiwell was coated with a small amount of optical adhesive. The silicon wafer-based multiwell was UV-postcured so that the well could be adhered to the silicon substrate tightly. To improve the mechanical stability, solvent resistance, and adhesion to silicon, thermal curing was also applied at 90°C for 12 h.

### FTIR microscopy

FTIR spectra along the points in each well were collected in the wave-number region 4000–650 cm<sup>-1</sup> with a Nicolet 6700 Continuum spectrometer (Thermo Fisher) equipped with a mercury cadmium telluride detector. The measurements were performed at a resolution of 8 cm<sup>-1</sup> by the averaging of 32 scans in a transmission mode. The spectral point-by-point mapping of the polymer surface in each well was performed with a computer-controlled microscope stage and Atlas mapping software (Thermo Fisher). A custom-built, temperature gradient stage, which could produce a temperature gradient of 30°C over 4 cm, was used to obtain the *in situ* FTIR spectra.<sup>18</sup> Before the dissolution test, a small piece of styrene-butadiene copolymer film (fabricated from a 5 wt % polymer solution in toluene)

was placed in each well of the silicon substrate and focused with the FTIR spectrometer. The solvent was introduced by the deposition of biodiesel into each well, at which point the dissolution process was assumed to have commenced.

### Molecular modeling

Molecular modeling was carried out with the Blends module of the Materials Studio 4.1 software package from Accelrys, Inc. (San Diego, CA). The platform used was a Dell Optiplex GX 270 PC with an Intel Pentium 4 (3.00-GHz) processor and 1.00 GB of RAM. These studies were conducted to evaluate the Flory–Huggins interaction parameters  $\chi_{FH}$  of the copolymers with methyl esters. The Flory–Huggins interaction parameter is an important indicator of thermodynamic compatibility. In the original Flory–Huggins theory,  $\chi_{FH}$  was given by<sup>19</sup>

$$\chi_{FH} = ZV_{\text{seg}} \frac{\Delta E_{\text{mix}}}{RT} \quad (1)$$

where  $\Delta E_{\text{mix}}$  is the energy of mixing per pair of monomers scaled by the unit volume,  $Z$  represents the lattice coordination number,  $V_{\text{seg}}$  is the volume of a mole of lattice sites,  $R$  is the gas constant, and  $T$  is the temperature (K). For off-lattice fluids, the coordination number loses some physical significance and becomes an adjustable parameter.<sup>20</sup> Methods to predict  $Z$  have been based on Monte Carlo packing algorithms that assume  $Z$  as the number of nearest neighbor segments for each segment.<sup>21,22</sup> The use of eq. (1) requires the prediction of the energy of mixing and assumes that the interaction parameter scales with reciprocal temperature. Computational techniques for the prediction of  $\chi_{FH}$ , such as the Blends module of Materials Studio, rely on predictions of the energy of mixing. In this study, the Blends module was used to predict the miscibility of the polymers with the individual components of the biodiesel.

### Shear viscosity measurements

The shear viscosity of the polymer/biodiesel solutions with concentrations of 5–20 wt % was measured with a rheometer (ARES-RFS, TA Instruments, New Castle, DE) in the temperature range 0–90°C. Steady-rate sweep tests were conducted for the shear viscosity measurements with continuous rotation to apply strain. The shear stress was monitored as a function of the shear rate, which was varied from 1 to 100 s<sup>-1</sup>. The shear-stress-to-shear-rate ratio yielded the steady shear viscosity.

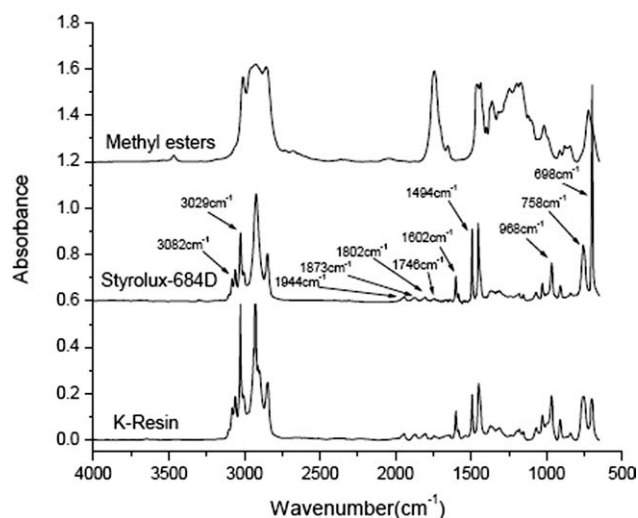


**Figure 1** IR spectra of the styrene–butadiene block copolymers and biodiesel.

### Mechanical tests

The tensile properties of the two styrene–butadiene copolymers and the PET samples were measured with an Instron 5569 testing machine (Instron Co., Canton, MA) according to ASTM D 638 and ASTM D 882. The drop-weight impact strength was determined with an Instron Dynatup 8200 drop-weight impact tester according to ASTM 7136. Five replicated specimens of each plastic were tested for each property. The resulting average data and their standard deviations were calculated and are reported.

## RESULTS AND DISCUSSION

### IR characterization of the styrene–butadiene block copolymers

The molecular structures of the styrene–butadiene block copolymers were revealed by FTIR spectroscopy, as shown in Figure 1. The spectra of the Styrolux and K-Resin samples were similar. The bands at 3082, 3029, and 968 cm<sup>-1</sup>, as shown in Figure 1, were assigned to CH (in =C–H) stretching and deformation vibrations, respectively, and thus represented the vinyl group in the butadiene segment. The characteristic bands of the phenol-ring CH deformation (at 1944, 1873, 1802, 1746, 758, and 698 cm<sup>-1</sup>) and ring CC stretching (at 1602 and 1494 cm<sup>-1</sup>) were also observed in the spectra, which indicated the presence of aromatic hydrocarbon (in the styrene segment). Other strong bands that were not indicated were mostly assigned to the vibrations of aliphatic groups from both the butadiene and styrene segments. The detailed IR band assignment for the styrene–butadiene copolymers is shown in Table I. Among the bands mentioned previously, the vibration of ring quadrant stretching at 1602 cm<sup>-1</sup>, which did not overlap with any of the absorption

**TABLE I**  
Tentative Assignment of the IR Bands of the Styrene–Butadiene Block Copolymers

Wave numbers (cm <sup>-1</sup> )	Band assignment
3082 and 3029	$\nu$ (CH in =C–H)
2925	$\nu_{as}$ (CH <sub>2</sub> )
2850	$\nu_s$ (CH <sub>2</sub> )
1944, 1873, 1802, 1746, 758, and 698	$\delta$ (ring CH out of plane)
1640	$\nu$ (–C=C–)
1602 and 1494	$\nu$ (ring CC)
1453	$\delta$ (CH <sub>2</sub> or CH <sub>3</sub> )
968	$\delta$ (CH in =C–H)

$\nu$  = stretching;  $\nu_{as}$  = asymmetry stretching;  $\nu_s$  = symmetry stretching;  $\delta$  = deformation.

peaks of biodiesel (also shown in Fig. 1), has been used successfully to study the dissolution behavior of PS in biodiesel.<sup>11</sup> This band was used as the characteristic signature of the copolymer samples to study their dissolution kinetics in biodiesel.

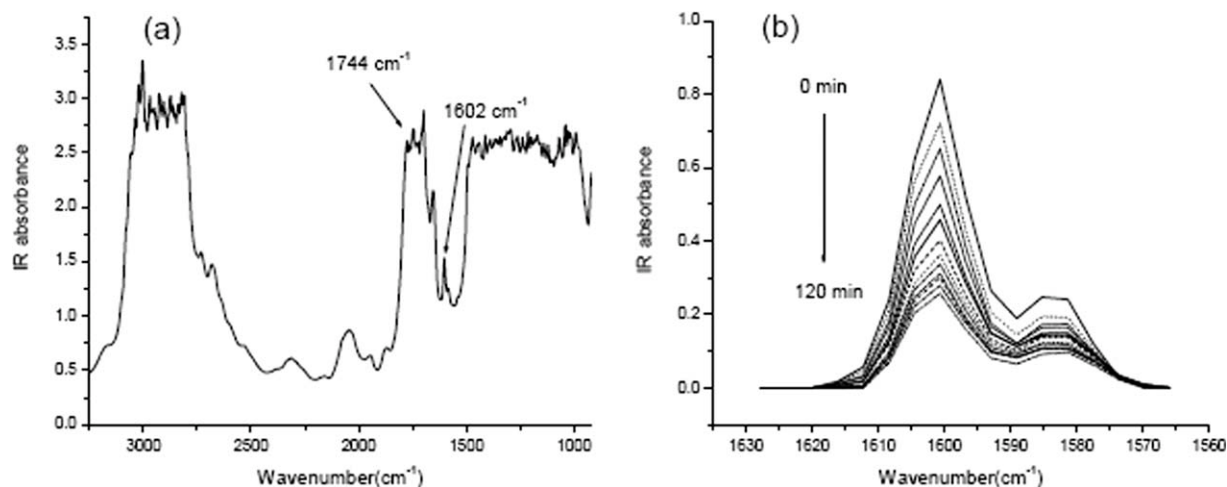
### Dissolution kinetics

The dissolution kinetics of the styrene–butadiene copolymer samples in biodiesel was studied by FTIR microscopy. For FTIR microscopy, the dissolution was carried out in multiwell substrates. The thiolene material that formed the wells has a high thermal stability and good solvent resistance,<sup>23</sup> which ensures that the dissolution can be conducted at high temperatures or in organic solvents. Another significant advantage of these microwells is the ease of prototyping new well designs for specific applications. More importantly, the multiwell substrate can be used to study polymer dissolution at high throughput. The multiwell design enables simultaneous analysis of large numbers of samples under

identical conditions. This high-throughput FTIR approach, based on a miniature sampling system, can significantly reduce the experimental time and increase the accuracy by minimizing variations between experiments. Certainly, fabricating larger numbers of arrays is possible and easily achieved if more variables or replicates are desired. In this study, 4 × 4 microwells were used, and the dissolution of the styrene–butadiene samples was studied as a function of temperature (with a custom-fabricated temperature gradient) with four replicates to obtain better statistics.

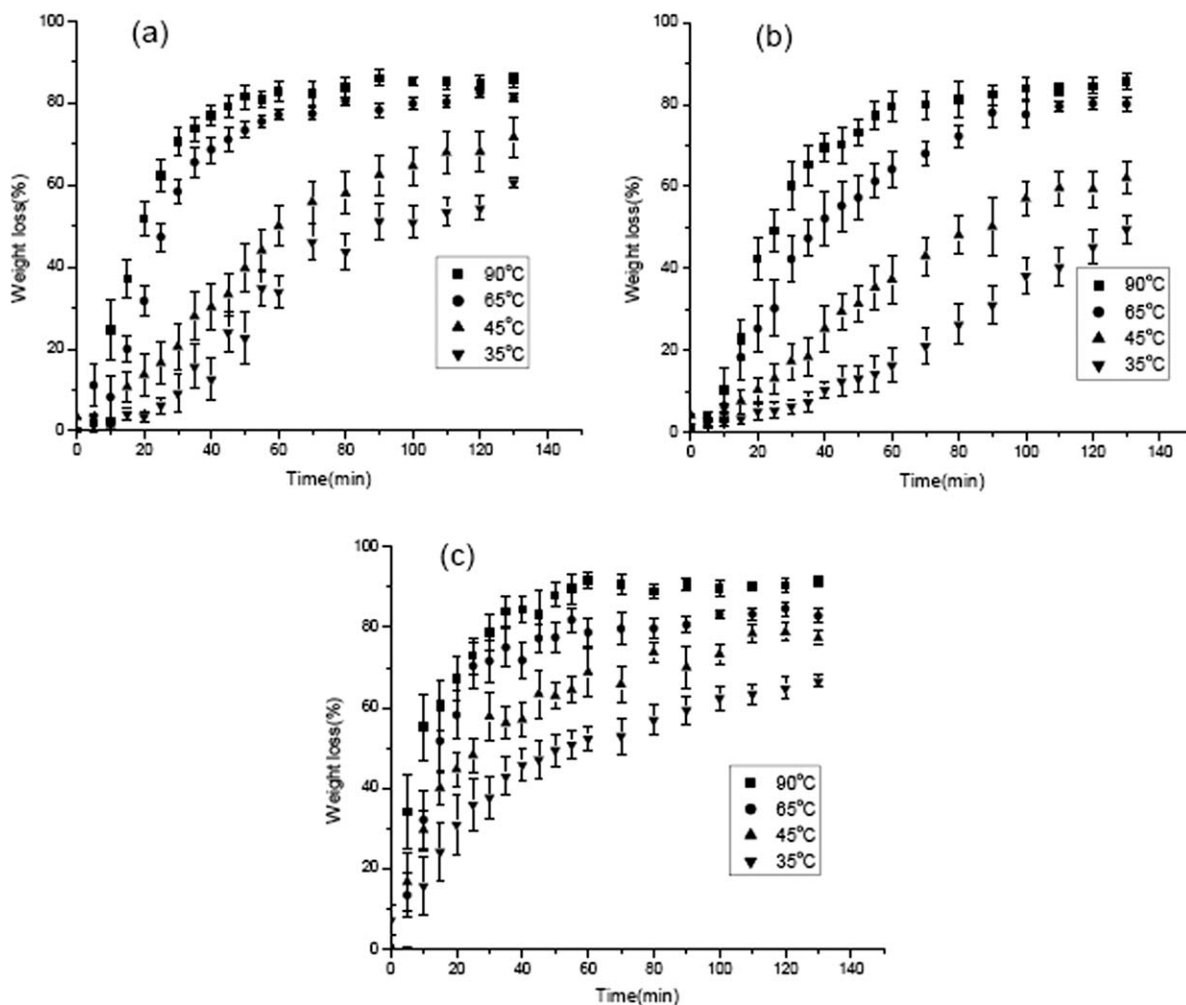
The dissolution of the styrene–butadiene copolymer samples (S1 and S2) was tracked by the change in their characteristic IR band at 1602 cm<sup>-1</sup>. Figure 2(a) shows a typical IR spectrum of an S1/biodiesel mixture at a dissolution time of 60 min. Despite the presence of strong absorbance bands due to the methyl esters, the characteristic peak at 1602 cm<sup>-1</sup> was easily discernable and could be quantitatively monitored. Thus, the dissolution kinetics could be obtained from the evolution of this band. Figure 2(b) displays the evolution of the IR absorbance of the 1602-cm<sup>-1</sup> band as a function of dissolution time. As expected, the absorbance decreased with dissolution time. Through the integration of the peak height of this band, the dissolution kinetics could be quantified.

Figure 3 shows the dissolution kinetics of the two styrene–butadiene block copolymers samples and PS films in biodiesel as a function of the dissolution temperature. The dissolution temperature was varied from 35 to 90°C with a custom-fabricated temperature gradient, as described before.<sup>18</sup> The results shown in Figure 3 reflect several important trends. First, all of the polymers exhibited faster dissolution kinetics with increasing temperature, as expected. Second, the two styrene–butadiene block copolymer



**Figure 2** (a) IR spectra of the Styrolux-684D biodiesel mixture at a dissolution time of 60 min and (b) change in the IR absorbance of the 1602-cm<sup>-1</sup> band as a function of dissolution time.





**Figure 3** Dissolution kinetics of the styrene–butadiene block copolymer and PS films as a function of the temperature as measured by FTIR microscopy: (a) Styrolux-684D, (b) K-Resin, and (c) PS.

samples [Fig. 3(a,b)] exhibited similar dissolution kinetics and temperature dependences. Third, both the styrene–butadiene block copolymer samples showed slower dissolution rates than the PS films [Fig. 3(c)]. This was attributed to the lower solubility of the butadiene segment of the copolymers in biodiesel. To validate the data obtained by high-throughput FTIR microscopy, conventional gravimetric studies were carried out (data not shown). The trends in the dissolution kinetics obtained from both methods were in excellent agreement; this demonstrated the validity of the high-throughput FTIR microscopy approach for dissolution testing. Our previous study<sup>11</sup> showed that there was a slight discrepancy between FTIR microscopy and gravimetry methods at long dissolution times, and this was attributed to the presence of dissolved mobile polymer in the multiwells in the path of the IR beam, which explained the plateau in the data at less than 100% dissolution. One can easily test large numbers of samples more repeatably with the FTIR microscopy method. Moreover, the samples in the multiwells could be diversified with the addition

of more variables, such as polydispersity or crystallinity of the polymer, or solvent blends. Furthermore, FTIR enables the *in situ* and simultaneous assessment of compositional changes and the diffusion or dissolution behaviors of individual components if a mixture of solvents or polymer blends (or copolymers) are used. All of these advantages make high-throughput FTIR microscopy a highly promising technique for studying polymer dissolution.

#### Activation energy ( $E_a$ ) of dissolution

The dissolution kinetics data shown in Figure 3 were used to calculate the  $E_a$  values of dissolution.  $E_a$  (kJ/mol) was given by the Arrhenius equation:

$$k_d = A \exp(-E_a/RT) \quad \text{or} \quad \ln k_d = -E_a/RT + \ln A \quad (2)$$

where  $k_d$  is the dissolution rate constant and  $A$  is a prefactor. Because  $E_a$  corresponds to the height of the potential barrier (sometimes called the *energy barrier*)

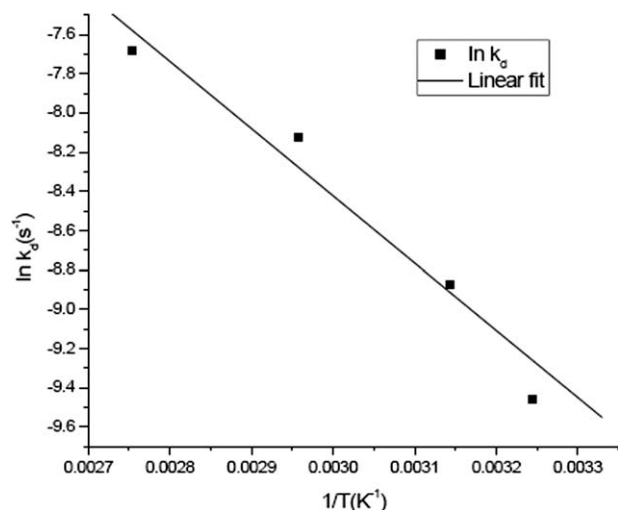


**Figure 4** Plot of  $\ln k_d$  versus the reciprocal temperature for Styrolux-684D.

for dissolution to occur, a higher  $E_a$  indicates that it is more difficult for the polymers to dissolve.  $k_d$  was obtained from the slope of the linear part of the dissolution kinetics data shown in Figure 3. By plotting  $\ln k_d$  versus reciprocal temperature, we obtained  $E_a$  from the slope of the resulting line, as shown in Figure 4 for S1. The calculated  $E_a$  values for the dissolution of both the styrene-butadiene block copolymers and PS in biodiesel are listed in Table II. It was clear that the  $E_a$  of the styrene-butadiene block copolymers was higher than that of PS. This result suggests that it was more difficult for the styrene-butadiene block copolymers to dissolve in biodiesel than PS, which was consistent with the dissolution kinetics data from the high-throughput FTIR method.

### Molecular modeling

The miscibility of polymer/solvent systems can be quantified by the Flory-Huggins interaction parameter. In this study, molecular dynamics simulations were carried out to calculate  $\chi$  between the styrene-butadiene copolymers and methyl esters, from which a better understanding could be acquired of the origin of the dissolution behavior. The homopolymers PS and polybutadiene were used with

**TABLE II**  
 $E_a$ 's of Dissolution for PS ( $M_n = 140$  kg/mol) and the Styrene-Butadiene Copolymers in Biodiesel

	S1	S2	PS
$E_a$ (kJ/mol)	28.5	28.8	22.4

**TABLE III**  
Calculated  $\chi$  Values Between Styrolux Polymers and Methyl Esters with the Blends Module of Materials Studio (at 298 K)

Styrolux copolymer versus methyl ester	$\chi$
Polybutadiene versus methyl linoleate	4.30
Polybutadiene versus methyl linolenate	3.38
Polybutadiene versus methyl oleate	4.04
Polybutadiene versus methyl palmitate	9.25
Polybutadiene versus methyl stearate	11.34
PS versus methyl linoleate	0.73
PS versus methyl linolenate	0.05
PS versus methyl oleate	0.96
PS versus methyl palmitate	5.82
PS versus methyl stearate	7.87

methyl esters in the  $\chi$  calculations to shed light on the contribution of each monomer species of the copolymer to the dissolution process. The Blends module was used to calculate the interaction energy, which was used to estimate the Flory-Huggins interaction parameter,  $\chi$ , as shown in eq. (1). Table III shows the calculated  $\chi$  values at 298 K for each of the polymers and the individual biodiesel components. The results indicate that the PS-methyl ester system had smaller  $\chi$  values compared to the polybutadiene-methyl ester system; this indicated that PS was more miscible with biodiesel. The data in Table III also indicate that the compatibility of methyl stearate and methyl palmitate (which made up  $\sim 15$  mol % of biodiesel) was the worst (i.e., high values of  $\chi$ ) with both polymers. These results clearly indicate that the slower dissolution kinetics (and higher  $E_a$ 's) of the styrene-butadiene copolymers could be attributed to the incompatibility of the butadiene segment of the copolymer with biodiesel components.

The relatively large  $\chi$  values predicted for some polymer/methyl esters systems (e.g., polybutadiene-methyl stearate, polybutadiene-methyl palmitate, PS-methyl palmitate, and PS-methyl stearate systems) in Table III did not necessarily imply the insolubility of styrene-butadiene copolymers in biodiesels. This was because both the styrene-butadiene copolymer and biodiesel were mixtures with various amounts of several components. The butadiene component only accounted for 15–30 wt % of the copolymer. Likewise, methyl palmitate and methyl stearate together made up about 15 mol % of biodiesel. In contrast, methyl oleate and methyl linoleate together made up greater than 75 mol % of biodiesel, and the  $\chi$  values were more reasonable in these cases. Another reason for the large  $\chi$  values in Table III is that the temperature at which these predictions were carried out was 298 K, which was lower than the experimental temperatures shown in Figure 3.

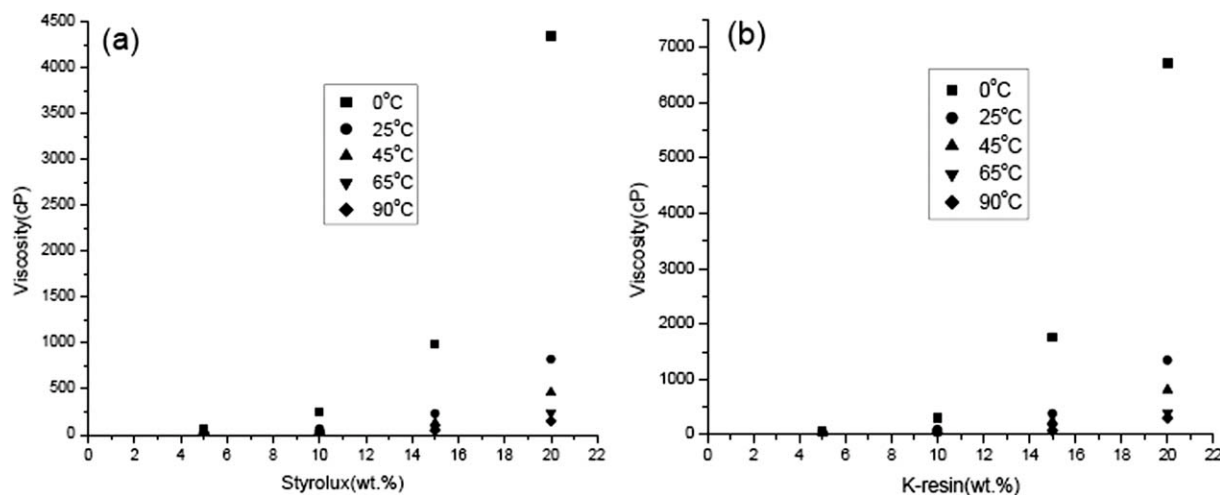


**Figure 5** Viscosities of the styrene–butadiene block copolymers in biodiesel as a function of the polymer concentration and temperature: (a) Styrolux-684D and (b) K-Resin. The shear rate was  $100 \text{ s}^{-1}$ .

### Shear viscosity

Because rheological properties, such as shear viscosity of fuel, are important for the performance of engines using polymer–biodiesel mixtures, measurements of shear viscosity for the styrene–butadiene copolymer solutions in biodiesel were carried out. These studies were performed as a function of polymer concentration and temperature. The results are shown in Figure 5. It is clear that the shear viscosity increased with polymer concentration and decreased with temperature. Furthermore, when these viscosities were compared to that of PS solutions (of a similar molecular weight),<sup>7</sup> we observed that at a given concentration and temperature, the viscosities of the styrene–butadiene copolymer solutions were lower than that of the PS solutions. It is likely that the softer butadiene segments in the styrene–butadiene copolymers contributed to the lower viscosity when dissolved in solvents. Because previous studies<sup>7</sup> have identified PS concentrations and temperatures that are suitable for use in diesel engines, it is likely that the styrene–butadiene copolymer solutions in those concentration and temperature ranges would also be suitable for use as fuels in diesel engines.

### Mechanical properties

The mechanical properties of the styrene–butadiene copolymers were measured and compared to that of PET. PET is widely used in synthetic fibers and beverage, food, and other liquid containers. However, it is not soluble in biodiesel. These comparative mechanical testing studies were conducted to investigate whether the styrene–butadiene copolymers had similar mechanical properties to PET with an eye toward the recycling of beverage bottles and food con-

tainers made of these materials for use as fuel in engines. In these studies, the tensile and impact testing properties were measured at room temperature. Table IV shows the mechanical properties of samples from bottles made of these three plastics. Both styrene–butadiene block copolymer samples displayed lower tensile and impact strengths (by a factor of 2) compared with PET. However, both copolymer samples showed greater toughness, as reflected by the tensile modulus and strain at break, which may enable more facile processing into complex three-dimensional shapes (e.g., for beverage bottles).

Combined with the ability of the styrene–butadiene block copolymers to dissolve in biodiesel under conditions that are suitable for their use as fuel in diesel engines, these materials may be promising environmentally friendly candidates to replace PET. Clearly, further studies are needed to determine the techno-economic feasibility of using these materials to make beverage bottles and other food containers. The studies described here lay the groundwork for future investigations on engine testing, product manufacturing, optimization of the dissolution behavior of the copolymers, and potential economic/environmental impact.

**TABLE IV**  
Mechanical Properties of the PET, Styrolux-684D, and K-Resin Bottles

	Tensile strength (MPa)	Tensile modulus (Young's; MPa)	Strain at break (%)	Impact strength (kJ/m <sup>2</sup> )
PET	87.2 ± 1.6	310.9 ± 6.0	35.3 ± 1.1	19.3 ± 0.3
Styrolux-684D	45.7 ± 0.9	160.2 ± 4.1	319.1 ± 11.2	7.9 ± 0.22
K-Resin	49.3 ± 0.8	179.0 ± 4.6	352.2 ± 14.0	10.9 ± 0.3

## CONCLUSIONS

The dissolution behavior of styrene–butadiene block copolymers in methyl esters was investigated with high-throughput FTIR microscopy. The dissolution kinetics of these copolymers were slower than that of neat PS. The dissolution behavior was studied as a function of temperature, and the  $E_a$  values of dissolution were calculated; consistent with the kinetics, these studies indicated that the styrene–butadiene block copolymers were harder to dissolve in biodiesel than PS. The experimental studies were complemented by molecular modeling calculations of thermodynamic polymer/solvent interaction parameters, which showed decreased compatibility of polybutadiene with the methyl ester components of biodiesel. The shear viscosity of the styrene–butadiene block copolymer/biodiesel solutions was measured to ascertain conditions under which these solutions could be used as engine fuel. Finally, the mechanical properties of the styrene–butadiene block copolymers were investigated, and it was shown that these materials had properties that were similar to those of PET. These results suggest that the styrene–butadiene block copolymers are promising environmentally friendly candidates to replace PET. These studies lay the groundwork for future investigations on engine testing, product manufacturing, optimization of the dissolution behavior of the copolymers, and potential economic/environmental impact.

The U.S. Government is authorized to reproduce and distribute reprints of this article for governmental purposes notwithstanding any copyright notation. The views and conclusions contained herein are those of the authors and should not be interpreted as necessarily representing the official policies or endorsements, either expressed or implied, of the U.S. Government. The authors acknowledge Michael Kessler and Wilber Lio for their help with the mechanical tests. They also acknowledge useful discussions with Marvin Schwedock (General Atomics, Inc.).

## References

1. Schwartz, S. S. *Plastics Materials and Processes*; Van Nostrand Reinhold: New York, 1982; p 44.
2. Rubin, I. I. *Handbook of Plastic Materials and Technology*; Wiley: New York, 1990; p 799.
3. U.S. Environmental Protection Agency. *Municipal Solid Waste Generation, Recycling, and Disposal in the United States: Facts and Figures for 2006*; Washington, DC, 2006.
4. U.S. Environmental Protection Agency. *Guide for Industrial Waste Management*; EPA 530-R-99-001; Washington, DC, 1999.
5. Williams, P. T. *Waste Treatment and Disposal*; Wiley: Chichester, England, 1988.
6. Nauman, E. B.; Lynch, J. C. U.S. Pat. 5,278,282 (1994).
7. Zhang, Y.; Mallapragada, S. K.; Narasimhan, B. *Polym Eng Sci*, 2010, 50, 863.
8. Tyson, K. S. *Biodiesel Handling and Use Guidelines*; U.S. Department of Energy, Energy Efficiency and Renewable Energy: Washington, DC, 2004.
9. Lacey, P. I.; Westbrook, S. R. SAE Tech Pap Ser 1995, 950248.
10. Knothe, G.; Steidley, K. R. *Energy Fuels* 2005, 19, 1192.
11. Zhang, Y.; Mallapragada, S. K.; Narasimhan, B. *Macromol Rapid Commun* 2010, 31, 385.
12. Gent, A. N.; Campion, R. P.; American Chemical Society Division of Rubber. *Engineering With Rubber: How to Design Rubber Components*; Hanser: Munich, 1992.
13. George, S. C.; Ninan, K. N.; Groeninckx, G.; Thomas, S. J *Appl Polym Sci* 2000, 78, 1280.
14. Bokobza, L. *Polym Int* 2000, 49, 743.
15. Cabral, J. T.; Hudson, S. D.; Harrison, C.; Douglas, J. F. *Langmuir* 2004, 20, 10020.
16. Harrison, C.; Cabral, J. T.; Stafford, C. M.; Karim, A.; Amis, E. J. *J. Micromech Microeng* 2004, 14, 153.
17. Vogel, B. M.; Cabral, J. T.; Eidelman, N.; Narasimhan, B.; Mallapragada, S. K. *J Comb Chem* 2005, 7, 921.
18. Thorstenson, J. B.; Petersen, L. K.; Narasimhan, B. *J Comb Chem* 2009, 11, 820.
19. Flory, P. J. *Principles of Polymer Chemistry*; Cornell University Press: Ithaca, NY, 1953.
20. Case, F. H.; Honeycutt, J. D. *Trends Polym Sci* 1994, 2, 259.
21. Fan, C. F.; Olafson, B. D.; Blanko, M.; Hsu, S. L. *Macromolecules* 1992, 25, 3667.
22. Kipper, M. J.; Seifert, S.; Thiyagarajan, P.; Narasimhan, B. *Polymer* 2004, 45, 3329.
23. Cabral, J. T.; Karim, A. *Meas Sci Technol* 2005, 16, 191.